IGSF6 is a biomarker associated with anti-tumor immune response in lung adenocarcinoma

Qisi Zheng
Nanjing Drum Tower Hospital Clinical College of Nanjing Medical University
Miao Li
Nanjing Drum Tower Hospital Clinical College of Nanjing Medical University
Gechen Jiang
Nanjing Drum Tower Hospital Clinical College of Nanjing Medical University
Jun Ni
Nanjing Drum Tower Hospital Clinical College of Nanjing Medical University
Han Shen
Nanjing Drum Tower Hospital Clinical College of Nanjing Medical University
Zhi Zhang
Jiangsu Cancer Hospital & Jiangsu Institute of Cancer Research & The Affiliated Cancer Hospital of Nanjing Medical University
Xinyu Tian (jipinxinyu@163.com)
Nanjing Drum Tower Hospital Clinical College of Nanjing Medical University

Research Article

Keywords: immunoglobulin superfamily 6, lung adenocarcinoma, prognosis, immune infiltration, macrophages

Posted Date: December 5th, 2022

DOI: https://doi.org/10.21203/rs.3.rs-2067836/v1

Abstract

Background: Immunoglobulin superfamily 6 (IGSF6) is a novel member of the immunoglobulin superfamily, and it is related to multiple diseases. However, the association of IGSF6 with the prognosis and anti-tumor immune response in lung adenocarcinoma (LUAD) remains unknown.

Results: By analyzing *IGSF6* expression in different cancers based on the pan-cancer data from The Cancer Genome Atlas (TCGA), it was found that *IGSF6* expression was decreased in LUAD. Results of quantitative-real-time-PCR (qRT-PCR), western-blot and immunohistochemistry (IHC) staining further confirmed this finding in paired tumor and normal tissues of LUAD patients. Meanwhile, promoter methylation level of *IGSF6*in LUAD samples increased compared to that in peritumor samples, implying a potential mechanism that leads to the aberrant expression of *IGSF6* in LUAD. By estimating the correlation between *IGSF6* expression and the prognosis of LUAD, we found that low *IGSF6* expression was significantly related to a worse survival rate. The enrichment analysis of *IGSF6* co-expression showed that *IGSF6* expression was closely associated with gene sets involved in immune cell proliferation and exogenous antigen presentation. In addition, high *IGSF6* expression was positively correlated with immune infiltrates with anti-tumor activity, including M1 macropahges, dendritic cells (DCs), and T helper 1 (Th1) cells. Finally, IGSF6 protein was indicated to be mainly located on the membrane of macrophages in LUAD, which might enable exogenous antigen uptake and presentation so as to regulate anti-tumor immune response.

Conclusions:IGSF6 is a biomarker for LUAD, which may promote the anti-tumor immune response leading to ameliorative prognosis.

Background

Lung cancer is the most common and lethal malignancy worldwide, resulting in over 2 million deaths each year [1, 2]. Most lung cancer patients present with advanced stages, and therapies with curative intent are often not available [3, 4]. As the most common subtype of lung cancer, LUAD is responsible for 50% of all lung cancer diagnoses, and its frequency is still increasing [5, 6]. At present, immunotherapy is a prominent strategy of treating various types of cancers including LUAD [7–10]. However, the effect of immunotherapy targeting LUAD is usually limited because of gene mutation, metabolic dysequilibrium, and immunosuppression [11, 12]. Thus, it is necessary to find specific immune-related biomarkers for LUAD and exploit them as new therapeutic targets.

IGSF6, also known as DOwn-Regulated by Activation (DORA), is a novel member of the immunoglobulin superfamily [13, 14]. Human IGSF6 gene is located at 16p11-p12, and its transcript level is high in spleen, lymph node and peripheral blood lymphocytes, while it is low in bone marrow, thymus, fetal liver and appendix [13, 15, 16]. IGSF6 protein was initially identified as a receptor of the CD8 family containing a single V type loop domain with an associated J chain region, a transmembrane region with an atypical tyrosine residue, and a cytoplasmic domain with three putative tyrosine phosphorylation sites. Current

studies confirm that IGSF6 expression in cells is committed to the myeloid lineage and perhaps acts as a co-receptor in the antigen uptake complex of DCs [13, 14]. Moreover, IGSF6 gene is associated with different diseases such as inflammatory bowel disease, atherosclerosis and Parkinson's disease [17–20]. However, the role of IGSF6 in LUAD progression and anti-tumor immune response is still unclear.

In the present study, we analyzed the *IGSF6* expression in different cancers based on TCGA data, and its correlation with the prognosis of LUAD. The association of *IGSF6* expression with molecular pathways in LUAD was further analyzed. Since both IGSF6 expression and potential function are closely related to immune cells, the correlation between *IGSF6* expression and immune infiltrates in the distinct tumor microenvironment of LUAD has also been measured. In addition, we also uncovered the critical involvement of IGSF6 in the anti-tumor activity of macrophages in LUAD.

Results

IGSF6 expression was decreased in LUAD

RNA-seq data of different cancers from TCGA were used to investigate the IGSF6 expression in tumor and surrounding healthy tissues. According to the tumor immune estimation resource, version 2 (TIMER2.0), IGSF6 was indicated to be differently expressed in multiple tumors. It was identified that IGSF6 expression was increased in cancers such as bladder urothelial carcinoma (BLCA), esophageal carcinoma (ESCA) and glioblastoma multiforme (GBM), and was decreased in some other cancers including LUAD, lung squamous cell carcinoma (LUSC), colon adenocarcinoma (COAD), pancreatic adenocarcinoma (PAAD), and rectum adenocarcinoma (READ), compared with that in peritumor normal tissues (Fig. 1A). To identify the results in LUAD, gene expression profiling interactive analysis 2 (GEPIA2) was used to examine 594 samples from the TCGA database. As shown, IGSF6 expression in LUAD samples (n = 535) was substantially lower than that in normal samples (n = 59) (Fig. 1B). By further comparison with matching normal tissues, IGSF6 expression was confirmed to be decreased in LUAD samples (n = 57) (Fig. 1C). Results of qRT-PCR and western-blot verified this finding (Fig. 1D-E). IHC images generated from the Human Protein Atlas (HPA) showed that IGSF6 protein was almost undetectable in LUAD samples (Fig. 1F). In addition, the the area under curve (AUC) of receiver operating characteristic (ROC) curve was 0.740 (95% CI 0.688–0.791) for IGSF6 in LUAD (Fig. 1G). The above results indicate that IGSF6 mRNA and protein levels are obviously decreased in LUAD tissues and may be a potential diagnostic biomarker for LUAD.

IGSF6 expression is associated with the LUAD clinicopathological parameters

Clinical-pathological parameters in LUAD patients, such as sample type (normal/primary tumor), tumor stage (stage 1, 2, 3, and 4), and lymph node stage (N 0, 1, 2, and 3), were analyzed by using UALCAN (Fig. 2 and Fig. S1A). Compared to that in normal samples, IGSF6 expression was much lower in primary

LUAD samples (Fig. 2A). The analysis of cancer stages showed that IGSF6 expression at all cancer stages was lower than normal, suggesting the potential association of IGSF6 expression with LUAD susceptibility (Fig. 2B). Similarly, IGSF6 expression in lymph node stage samples of LUAD was markedly lower than normal, indicating that IGSF6 is absent from malignancy (Fig. 2C). We also found that IGSF6 expression in LUAD was related to histological subtypes (Fig. 2D). These data further verify that IGSF6 may be a potential biomarker for the early diagnosis of LUAD.

To identify the potential mechanism leading to decreased IGSF6 expression in LUAD, we estimated the promoter methylation level of IGSF6 in normal tissues and primary tumors by applying UALCAN. Results indicated that promoter methylation level of IGSF6 increased significantly in primary LUAD tissues compared with that in normal tissues (Fig. 3A-C and Fig. S1B). Meanwhile, it was also suggested that IGSF6 mutation was unrelated to its aberrant expression in LUAD (Fig. 3D-E).

IGSF6 expression is negatively correlated with LUAD prognosis

To assess the utility of IGSF6 expression in predicting LUAD prognosis, the correlation between IGSF6 expression and survival rate in the TCGA cohort was analyzed. Results showed that lower IGSF6 expression was significantly linked with poor overall survival (OS) (HR = 0.64, p = 0.003) (Fig. 4A), disease special survival (DSS) (HR = 0.63, p = 0.013) (Fig. 4B), and progress free interval (PFI) (HR = 0.76, p = 0.041) (Fig. 4C), suggesting that IGSF6 is a potential biomarker of LUAD prognosis. Meanwhile, IGSF6 mutation was not related to the survival rate of LUAD patients (Fig. S2).

Correlation And Enrichment Analyses

To investigate the function and signaling pathways associated with IGSF6, the correlation analysis between IGSF6 and all the other mRNAs in LUAD was performed based on TCGA data. Top 300 genes related to IGSF6 were selected for enrichment analysis, in which the top 50 genes were displayed in a heatmap (Fig. 5A). To further explore potential functional pathways associated with IGSF6 in LUAD, Gene Ontology (GO) functional enrichment analysis was performed based on the top 300 genes using the R software clusterProfiler package. Analysis of biological processes (BP) indicated that immune cell proliferation might be the most related biological process of IGSF6 in LUAD (Fig. 5B). Similar to previous studies, cell component (CC) analysis predicted that IGSF6 was mainly located on the plasma membrane and was closely associated with major histocompatibility complex class II (MHCII) (Fig. 5C). Molecular function (MF) analysis showed that molecular function of IGSF6 was closely related to receptor activity (Fig. 5D). Kyoto Encyclopedia of Genes and Genomes (KEGG) analysis indicated that IGSF6 was the most related to phagosome formation pathway, which is essential for exogenous antigen uptake and presentation by DCs and macrophages (Fig. 5E). In addition, gene set enrichment analysis (GSEA) analysis showed that gene sets of cytokine-receptor interaction and intercellular interaction were

significantly enriched (Fig. 5F). These results indicate that IGSF6 may be a receptor that is involved in pathways controlling immune cell proliferation and exogenous antigen presentation in LUAD.

IGSF6 expression is closely related to immune infiltrates in LUAD

Antigen presentation and immune cell proliferation in tumor microenvironment are crucial for the priming of anti-tumor immune response [21, 22]. And, IGSF6 is restricted to immune system tissues [13, 14]. Hence, both TISIDB and TIMER2.0 databases were used to analyze the association of immune cell infiltration with IGSF6 expression in LUAD. We firstly confirmed that IGSF6 expression was adversely correlated with the purity of LUAD (Fig. S3), so as to eliminate interference of the tumor purity on the study of immune infiltration. Infiltration scores of immune cells with anti-tumor activity were higher in the high-IGSF6 cohort compared with those in the low-IGSF6 cohort (Fig. 6A). Meanwhile, we found that high IGSF6 expression was the most relevant to M1 macrophage, DC and Th1 infiltration (Fig. 6B-C, Fig. 7 and Fig. S3A-B). In addition, IGSF6 expression was negatively correlated with immunosuppressive cell infiltration including M2 macrophages, regulatory T cells (Tregs) and myeloid-derived suppressor cells (MDSCs) (Fig. S3C-E), indicating that high IGSF6 expression is closely related to anti-tumor immune infiltrates in LUAD.

IGSF6 expression is positively correlated with the anti-tumor activity of macrophages in LUAD

Antigen peptide-MHCII complex presented by professional antigen presenting cells (APCs) including DCs, macrophages and B cells is essential for the activation of Th1 cells [23–25]. The above correlation and enrichment analyses identified that IGSF6 was strongly linked with MHCII complex and might participate in antigen uptake by macrophages and DCs through acting as a co-receptor. Besides that, previous studies have also supposed a potential function of IGSF6 as a co-receptor, perhaps in an antigen uptake complex, or in homing or recirculation of DCs [13], which further implies the importance of IGSF6 in exogenous antigen presentation by APCs. Moreover, we analyzed the IGSF6 level in single cell of lung tissue and found that IGSF6 was predicted to be the most abundant in macrophages (Fig. 8A-B). Subcellular localization analysis predicted that IGSF6 might be located on the plasma membrane of macrophages, which was further confirmed by FCM (Fig. 8C-E). The analysis of structure and association networks found that IGSF6 was closely related to complement and coagulation cascades that can promote macrophages to engulf pathogens for antigen presentation (Fig. 8F-G). Taken together, it is suggested that IGSF6 may enhance the exogenous antigen uptake and presentation by macrophages in LUAD, thereby leading to the activation and proliferation of Th1 cells. To ensure this hypothesis, we examined the relationship between IGSF6 level and the expression of genes encoding M1 and Th1 effector molecules. The results showed that IGSF6 expression was positively correlated with M1 and Th1

effector molecules (Fig. 9), suggesting that IGSF6 is significantly related to M1-associated anti-tumor immune response in LUAD.

Discussion

IGSF6 is a novel member of the immunoglobulin superfamily, which belongs to the CD8 family of receptors and perhaps functions as a co-receptor [13]. Human IGSF6 gene spans 12 kb with six exons arranged in a manner similar to other members of the IGSF. Expression of IGSF6 gene is restricted to cells of the immune system, and the human IGSF6 gene is expressed as two mRNAs of 1 and 2.5 kb [14, 16]. IGSF6 gene has been identified as a candidate for the susceptibility of different diseases [17, 26]. However, the role of IGSF6 in immune engagement during LUAD development is still unknown.

In the present study, the *IGSF6* expression in different tumors was analyzed, and we found that *IGSF6* expression was significantly decreased in 4 types of cancers including LUAD. Through the analysis of TCGA LUAD data sets, the *IGSF6* expression in LUAD tissues was significantly lower than that in normal tissues. IGSF6 levels in LUAD samples and normal samples were further verified by IHC from HPA database, qRT-PCR, and western-blot. ROC curve was used to evaluate the potential of *IGSF6* in predicting LUAD, and we found that *IGSF6* had certain accuracy in predicting the outcome of LUAD. We also identified that low *IGSF6* expression was associated with the worse prognosis of LUAD, supposing that overexpression of IGSF6 may improve the prognosis of LUAD patients. Finally, *IGSF6* expression in LUAD tissues at all stages was lower than that in normal samples, suggesting that IGSF6 may serve as a marker for early diagnosis of LUAD. Interestingly, methylation level of *IGSF6* promoter in LUAD tissues increased compared to that in normal samples, suggesting that DNA methylation may be the cause of *IGSF6* aberrant expression in LUAD.

Next to this, top 300 genes co-expressed with *IGSF6* in LUAD were selected for enrichment analysis. GO enrichment analysis indicated that the co-expression of *IGSF6* was primarily associated with immune cell proliferation and MHCII-involved antigen presentation. KEGG pathway analysis showed that the co-expression of *IGSF6* was closely related to phagosome formation, which is essential for exogenous antigen presentation by APCs. The GSEA enrichment analysis showed that gene sets grouped according to *IGSF6* expression were mainly enriched in cytokine-receptor interaction and intercellular interaction. It has been well established that antigen peptide-MHCII complex presented by macrophages and DCs is essential for the activation of Th1 cells [27–30]. Previous studies have also proposed that IGSF6 may be closely related to antigen uptake, or the recirculation of DCs [13]. Therefore, it is implied that IGSF6 may be important for antigen uptake and presentation by macrophages and DCs in LUAD.

The analysis of immune cell infiltration in LUAD indicated that *IGSF6* was positively correlated with immune cell infiltration with anti-tumor activity such as M1 macrophages, DCs and Th1 cells, and was negatively correlated with immunosuppressive cell infiltration including M2 macrophages, Tregs and MDSCs. By applying HPA database, IGSF6 was predicted to be the most abundant in macrophages from lung tissue, and we confirmed the localization of IGSF6 on the plasma membrane of macrophages in

LUAD. In addition, the following association networks verified that IGSF6 was closely related to complement and coagulation cascades that can promote macrophages to engulf pathogen for antigen presentation. Taken together, IGSF6 may accelerate the exogenous antigen presentation by macrophages in LUAD, thereby leading to the activation and proliferation of Th1 cells. And we did found that *IGSF6* expression was positively correlated with M1 and Th1 effector molecules, supposing that IGSF6 is associated with M1-induced anti-tumor immune response in LUAD. However, the accurate role of IGSF6 in regulating the antigen presentation process of macrophages still needs further investigations. Besides that, we found that the proportion of $IGSF6^{+}$ macrophages decreased in LUAD tissues compared with that in adjacent normal tissues, which may be caused by the following mechanisms: (1) In tumor microenvironment, IGSF6 participates in the exogenous antigen uptake by M1 and migrates inside the cells with the exogenous antigen, leading to the decrease of IGSF6 level on cell surface; (2) IGSF6 is mainly expressed on M1. In tumor microenvironment, macrophages are mainly polarized to M2 type to promote the tumor escape, which results in the decrease of M1 population with IGSF6 expression.

Conclusions

The present study indicated that *IGSF6* expression was deceased in LUAD, and its expression was correlated with clinical case characteristics and prognosis of LUAD. IGSF6 was significantly related to the extent of immune infiltrates in LUAD, which may enhance the M1-induced anti-tumor effect. Therefore, IGSF6 is a potential biomarker for the diagnosis, treatment and prognosis of LUAD.

Methods

Data Collection and Analysis

TIMER2.0 (http://timer.cistrome.org/) was used to analyze the differential expression of *IGSF6* between tumor and adjacent normal tissues across all TCGA tumors. To measure *IGSF6* expression in LUAD, data of tumor tissues and normal tissues was obtained from the TCGA database and determined by GEPIA2 (http://gepia2.cancer-pku.cn/#index).

Ihc Staining

IHC images of IGSF6 protein level in normal tissues and LUAD tissues were downloaded from the HPA (http://www.proteinatlas.org/).

Patients And Samples

Paired tumor tissues and adjacent normal tissues were collected from LUAD patients (n = 9) who underwent primary surgical resection. The present study was approved by the respective Ethics

Committee of Nanjing Drum Tower Hospital Clinical College of Nanjing Medical University. Written informed consent was obtained from all the subjects in accordance with the Declaration of Helsinki.

Rna Isolation And Qrt-pcr

Total RNA was extracted from cells with TRIzol reagent (Invitrogen, California) following the manufacturer's instructions. Random primers and a ReverTra Ace® qPCR RT Kit (Toyobo, Osaka, Japan) were used to synthesize cDNA. Bio-Rad SYBR Green Supermix (Bio-Rad, Hercules) was used to perform quantitative real-time PCR in triplicate. The primer sequences were as follows: human *β-ACTIN*, sense 5-GAGTGTGGAGACCATCAAGGA-3, antisense 5-TGTATTGCTTTGCGTTGGAC-3; human *IGSF6*, sense 5-GCAATCTCGGCTCACTACAACCTC-3, antisense 5-CGTGGTGGTGCGTACCTGTAATC-3. The $2^{-\Delta CT}$ calculation method was used to determine the relative target gene level.

Western-blot

Protein extracted from tissues was prepared as described previously [31]. Protein (300 μg) was separated by 12% SDS-PAGE and then transferred onto Immobilon polyvinylidene fluoride membranes (BioRad, Hercules, CA). The membranes were blocked with 30 mL 5% BSA before probing overnight at 4°C with rabbit-anti-human IGSF6 polyclonal antibody (1:1000) (ThermoFisher Scientific, Dallas, TX) or rabbit-anti-human β-ACTIN antibody (1:1000) (CST, Danvers, MA) and then with a secondary HRP-conjugated goat anti-rabbit IgG (diluted at 1:8000) (CST, Danvers, MA), followed by chemiluminescent detection (Champion Chemical, Whittier, CA). Full-length blots are included in the Supplementary Information file.

Ualcan Analysis

The UALCAN (http://ualcan.path.uab.edu/) website provides an extensive and interactive study of bioinformatics applying RNA-seq and clinical data of 33 malignancies from TCGA. The database can compare gene expression and promoter methylation level in tumors to those in healthy samples, and in different tumor stages or subtypes, as well as other clinicopathological features. In the present study, *IGSF6* expression level and promoter methylation level from major clinical features such as tissue type (normal/primary tumor), LUAD stage (stages 1, 2, 3, and 4), and lymph node stage (N0, 1, 2, and 3) were analyzed by using UALCAN.

Survival Prognosis Analysis

Kaplan-Meier survival curves were used to assess the OS, DSS, and PFI of *IGSF6* in LUAD. Survival curves comparing the *IGSF6*-mutated and *IGSF6*-unmutated groups in LUAD were obtained from cBioPortal (https://www.cbioportal.org/). Cutoff-high (50%) and cutoff-low (50%) values were used as the expression thresholds for splitting the high-expression and low-expression cohorts. The hazard ratio (HR)

with 95% confidence intervals was also analyzed, as well as the log-rank *p*-value. Statistical significance was defined as $p < 0.05$.

IGSF6 **-Related Gene Enrichment Analysis**

Pearson correlation analysis of IGSF6 mRNA and other mRNAs in LUAD was performed using TCGA LUAD data. The 300 genes that were the most relevant to *IGSF6* were selected for enrichment analysis to determine the potential function of IGSF6. GO and KEGG analyses were conducted by running the R software *clusterProfiler* package. Different gene expression between the high- and low-risk subgroups were identified (|log2FC|>1, FDR < 0.05). The Benjamini-Hochberg (BH) method was used to adjust the *p* value. Detailed parameters were shown as the following: *ont* = all, *qvalue-Cutoff* = 0.05, and *pvalue-Cutoff* = 0.05. GSEA was performed using the gseKEGG and gsePathway functions in *clusterProfiler* with the following parameters: *maxGSSize* = 1000, *minGSSize* = 10, *nPerm* = 1000, and *pvalue-Cutoff* = 0.05.

Immune Cell Infiltration

TISIDB (http://cis.hku.hk/TISIDB/index.php) is an online platform that combines various heterogeneous data sources to study tumor and immune system interactions. This database may help researchers understand how tumors and immune cells interact, as well as forecast immunotherapy responses and identify new immunotherapy targets. In the present study, TISIDB was utilized to investigate the association of *IGSF6* with tumor infiltrating lymphocytes (TILs) in LUAD. In addition, Timer2.0 was used to analyze the correlation between *IGSF6* and suppressive immune infiltrates including M2 macrophages, Tregs and MDSCs.

Prediction Of Igsf6 Localization In Cells

Analysis of cell type which is enriched with IGSF6 protein in lung, as well as prediction of IGSF6 localization in cells, was obtained from the HPA database.

Flow Cytometry (Fcm)

Collagenase II (Sigma-Aldrich, St. Louis, MO) was used to digest tumor tissues and adjacent tissues derived from LUAD patients to obtain a single-cell suspension. Mononuclear cells were isolated by density gradient centrifugation over a Ficoll cushion. Cells were collected and stained with PE-anti-human-CD68 (eBioscience, San Diego, CA), APC-anti-human-CD80 (eBioscience, San Diego, CA) and FITC-anti-human-IGSF6 (Epigentek, Farmingdale, NY) mAbs. Stained cells were collected and then analyzed via FCM (FACSAria, BD Biosciences).

Statistical Analysis

Statistical analysis of defining group differences is determined by two-tailed *t* test comparing two groups, one-way or two ways ANOVA multiple tests comparing three or more groups. ROC curve was used to analyze the sensitivity and specificity of *IGSF6* in the diagnosis of LUAD by estimating AUC. The Wilcoxon test was used to compared the *IGSF6* expression in wild-type (WT) and *IGSF6*-mutated groups of LUAD. In survival curves, HR and *p*-values were described using log-rank test. Spearman's correlation coefficient was calculated to analyze the association of *IGSF6* expression with immune infiltrates. Pearson correlation coefficient was calculated to analyze the connection between *IGSF6* expression and other molecules. The strength of correlation was judged to be a very weak correlation if $r < 0.2$, weak if $r < 0.4$, moderate if $r < 0.6$, strong if $r < 0.8$, and very strong if $r < 1.0$. Statistical significance was defined as $p < 0.05$.

Abbreviations

IGSF6, Immunoglobulin superfamily 6; LUAD, lung adenocarcinoma; TCGA, The Cancer Genome Atlas; qRT-PCR, quantitative-real-time-PCR; IHC, immunohistochemistry; DCs, dendritic cells; Th1, T helper 1; DORA, DOwn-Regulated by Activation; BLCA, bladder urothelial carcinoma; ESCA, esophageal carcinoma; GBM, glioblastoma multiforme; LUSC, lung squamous cell carcinoma; COAD, colon adenocarcinoma; PAAD, pancreatic adenocarcinoma; READ, rectum adenocarcinoma; MHCII, major histocompatibility complex class II; MF, Molecular function; APCs, antigen presenting cells; TIMER2.0, Tumor immune estimation resource, version 2; GEPIA2, gene expression profiling interactive analysis 2; HPA, Human Protein Atlas; OS, overall survival; DSS, disease specific survival; PFI, progress free interval; GO, Gene Ontology; KEGG, Kyoto Encyclopedia of Genes and Genomes; BH, Benjamini-Hochberg; GSEA, gene set enrichment analysis; TILs, tumor infiltrating lymphocytes; Tregs, regulatory T cells; MDSCs, myeloid-derived suppressor cells; ROC, receiver operating characteristic; AUC, the area under curve; WT, wild-type.

Declarations

Ethics approval and consent to participate

The present study was approved by the respective Ethics Committee of Nanjing Drum Tower Hospital Clinical College of Nanjing Medical University. Written informed consent was obtained from all the subjects in accordance with the Declaration of Helsinki.

Consent for publication

Not applicable.

Availability of data and materials

All data generated or analysed during this study are included in this published article and its supplementary information files.

Competing interests

The authors declare that they have no competing interests.

Funding

This work was supported by the National Natural Science Foundation of China (Grant No. 81802855), the Natural Science Foundation of Jiangsu Province (Grant No. BK20180123), the Jiangsu Postdoctoral Research Foundation (Grant No. 2018K253C), and the China Postdoctoral Science Foundation (Grant No. 2018ZM642225).

Authors' contributions

XT, QZ, and JN conceived the presented ideas and researched the background of the study. QZ, GJ, and HS prepared the figures and tables. QZ, ZZ, and GJ wrote the manuscript. All authors contributed to the article and approved the submitted version.

Acknowledgements

Not Applicable.

References

1. Sung H, Ferlay J, Siegel RL, Laversanne M, Soerjomataram I, Jemal A, et al. Global Cancer Statistics 2020: GLOBOCAN Estimates of Incidence and Mortality Worldwide for 36 Cancers in 185 Countries. CA Cancer J Clin. 2021; 71: 209-249.
2. Siegel RL, Miller KD, Fuchs HE, Jemal A. Cancer Statistics, 2021. CA Cancer J Clin. 2021; 71: 7-33.
3. Li MY, Liu LZ, Dong M. Progress on pivotal role and application of exosome in lung cancer carcinogenesis, diagnosis, therapy and prognosis. Mol Cancer. 2021; 20: 22.
4. Deb D, Moore AC, Roy UB. The 2021 Global Lung Cancer Therapy Landscape. J Thorac Oncol. 2022; 17: 931-936.
5. Brody H. Lung cancer. Nature. 2020; 587: S7.
6. Relli V, Trerotola M, Guerra E, Alberti, S. Abandoning the Notion of Non-Small Cell Lung Cancer. Trends Mol Med. 2019; 25: 585-594.
7. Topper MJ, Vaz M, Chiappinelli KB, DeStefano-Shields CE, Niknafs N, Yen RC, et al.Epigenetic Therapy Ties MYC Depletion to Reversing Immune Evasion and Treating Lung Cancer. Cell. 2017; 171: 1284-1300 e21.
8. Scalera S, Mazzotta M, Corleone G, Sperati F, Terrenato I, Krasniqi E, et al. KEAP1 and TP53 Frame Genomic, Evolutionary, and Immunologic Subtypes of Lung Adenocarcinoma With Different Sensitivity to Immunotherapy. J Thorac Oncol. 2021; 16: 2065-2077.

9. Dong ZY, Zhong WZ, Zhang XC, Su J, Xie Z, Liu SY, et al. Potential Predictive Value of TP53 and KRAS Mutation Status for Response to PD-1 Blockade Immunotherapy in Lung Adenocarcinoma. Clin Cancer Res. 2017; 23: 3012-3024.
10. Dobosz P, Dzieciatkowski T. The Intriguing History of Cancer Immunotherapy. Front Immunol. 2019; 10: 2965.
11. Hegde PS, Chen DS. Top 10 Challenges in Cancer Immunotherapy. Immunity. 2020; 52: 17-35.
12. Mamdani H, Matosevic S, Khalid AB, Durm G, Jalal SI. Immunotherapy in Lung Cancer: Current Landscape and Future Directions. Front Immunol. 2022; 13: 823618.
13. Bates EE, Dieu MC, Ravel O, Zurawski SM, Patel S, Bridon JM, et al. CD40L activation of dendritic cells down-regulates DORA, a novel member of the immunoglobulin superfamily. Mol Immunol. 1998; 35: 513-524.
14. Bates EE, Kissenpfennig A, Peronne C, Mattei MG, Fossiez F, Malissen B, et al. The mouse and human IGSF6 (DORA) genes map to the inflammatory bowel disease 1 locus and are embedded in an intron of a gene of unknown function. Immunogenetics. 2000; 52: 112-120.
15. Shu KX, Wu LX, Xie YF, Zhao JF, Liang YL, Li B. Characterization of the human PAP1 gene and its homologue possible involvement in mouse embryonic development. Colloids Surf B Biointerfaces. 2006; 52: 22-30.
16. Tassano E, Ronchetto P, Calcagno A, Fiorio P, Gimelli G, Capra V, et al. 'Distal 16p12.2 microdeletion' in a patient with autosomal recessive deafness-22. J Genet. 2019; 98.
17. King K, Moody A, Fisher SA, Mirza MM, Cuthbert AP, Hampe J, et al. Genetic variation in the IGSF6 gene and lack of association with inflammatory bowel disease. Eur J Immunogenet. 2003; 30: 187-190.
18. Cui S, Sun H, Gu X, Lv E, Zhang Y, Dong P, et al. Gene expression profiling analysis of locus coeruleus in idiopathic Parkinson's disease by bioinformatics. Neurol Sci. 2015; 36: 97-102.
19. Shen Y, Xu LR, Tang X, Lin CP, Yan D, Xue S, et al. Identification of potential therapeutic targets for atherosclerosis by analysing the gene signature related to different immune cells and immune regulators in atheromatous plaques. BMC Med Genomics. 2021; 14: 145.
20. Li Z, Chyr J, Jia Z, Wang L, Hu X, Wu X, et al. Identification of Hub Genes Associated with Hypertension and Their Interaction with miRNA Based on Weighted Gene Coexpression Network Analysis (WGCNA) Analysis. Med Sci Monit. 2020; 26: e923514.
21. Lee MY, Jeon JW, Sievers C, Allen CT. Antigen processing and presentation in cancer immunotherapy. J Immunother Cancer. 2020; 8.
22. Hernandez-Malmierca P, Vonficht D, Schnell A, Uckelmann HJ, Bollhagen A, Mahmoud MAA, et al. Antigen presentation safeguards the integrity of the hematopoietic stem cell pool. Cell Stem Cell. 2022; 29: 760-775 e10.
23. Hong S, Zhang Z, Liu H, Tian M, Zhu X, Zhang Z, et al. B Cells Are the Dominant Antigen-Presenting Cells that Activate Naive CD4(+) T Cells upon Immunization with a Virus-Derived Nanoparticle Antigen. Immunity. 2018; 49: 695-708 e4.

24. Fu Y, Zhan X, Wang Y, Jiang X, Liu M, Yang Y, et al. NLRC3 expression in dendritic cells attenuates CD4(+) T cell response and autoimmunity. EMBO J. 2019; 38: e101397.
25. Ma J, He P, Zhao C, Ren Q, Dong Z, Qiu J, et al. A Designed alpha-GalCer Analog Promotes Considerable Th1 Cytokine Response by Activating the CD1d-iNKT Axis and CD11b-Positive Monocytes/Macrophages. Adv Sci (Weinh). 2020; 7: 2000609.
26. Liu L, Yu Y, Hu LL, Dong QB, Hu F, Zhu LJ, et al. Potential Target Genes in the Development of Atrial Fibrillation: A Comprehensive Bioinformatics Analysis. Med Sci Monit. 2021; 27: e928366.
27. Wei W, Mu S, Han Y, Chen Y, Kuang Z, Wu X, et al. Gpr174 Knockout Alleviates DSS-Induced Colitis via Regulating the Immune Function of Dendritic Cells. Front Immunol. 2022; 13: 841254.
28. Nguyen HO, Schioppa T, Tiberio L, Facchinetti F, Villetti G, Civelli M, et al. The PDE4 Inhibitor Tanimilast Blunts Proinflammatory Dendritic Cell Activation by SARS-CoV-2 ssRNAs. Front Immunol. 2021; 12: 797390.
29. Han JC, Li QX, Fang JB, Zhang JY, Li YQ, Li SZ, et al. GII.P16-GII.2 Recombinant Norovirus VLPs Polarize Macrophages Into the M1 Phenotype for Th1 Immune Responses. Front Immunol. 2021; 12: 781718.
30. de Freitas ESR, Galvez RI, Pereira VRA, de Brito MEF, Choy SL, Lotter H, et al. Programmed Cell Death Ligand (PD-L)-1 Contributes to the Regulation of CD4(+) T Effector and Regulatory T Cells in Cutaneous Leishmaniasis. Front Immunol. 2020; 11: 574491.
31. Tian X, Zheng Y, Yin K, Ma J, Tian J, Zhang Y, et al. LncRNA AK036396 Inhibits Maturation and Accelerates Immunosuppression of Polymorphonuclear Myeloid-Derived Suppressor Cells by Enhancing the Stability of Ficolin B. Cancer Immunol Res. 2020; 8: 565-577.

Figures

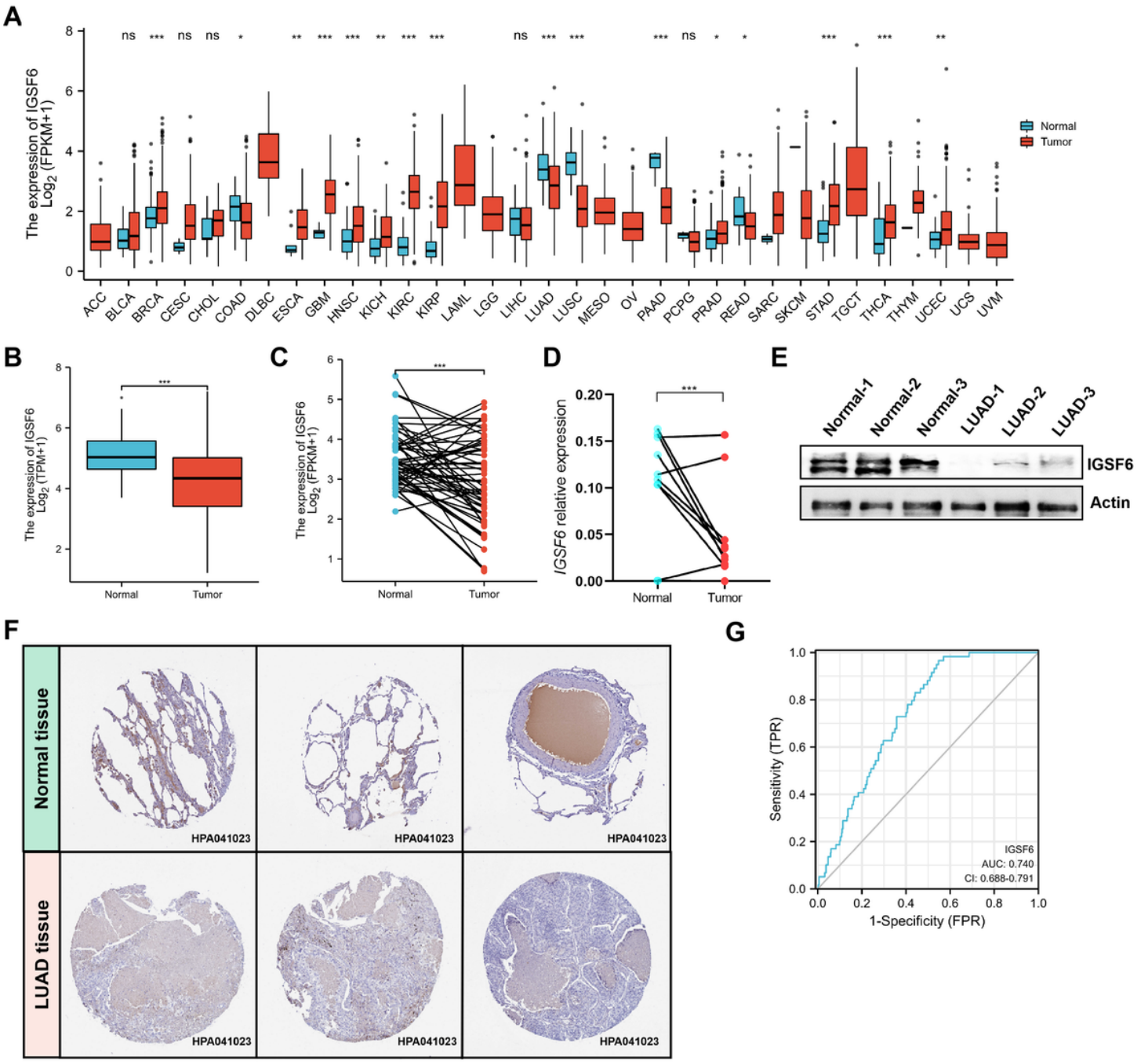

Figure 1

*IGSF6*expression was decreased in LUAD

(A) *IGSF6*expression in pan-cancer data of TCGA was determined by TIMER2.0. (B) *IGSF6*expression data in LUAD tissues and normal tissues from TCGA was analyzed by GEPIA2. (C) *IGSF6* expression in paired LUAD tissues and normal tissues from TCGA. (D) qRT-PCR was used to detect *IGSF6* expression in tumor tissues and paired normal adjacent tissues (n=9). (E) IGSF6 protein level in LUAD tissues and paired adjacent normal tissues was measured by western-blot (n=3). (F) IHC images of IGSF6 protein in normal tissues and LUAD tissues were obtained from HPA. (G) ROC curve analysis of *IGSF6* in LUAD patients. Data were shown as mean ± SD. *p<0.05, **p<0.01, ***p<0.001, ns: no significance.

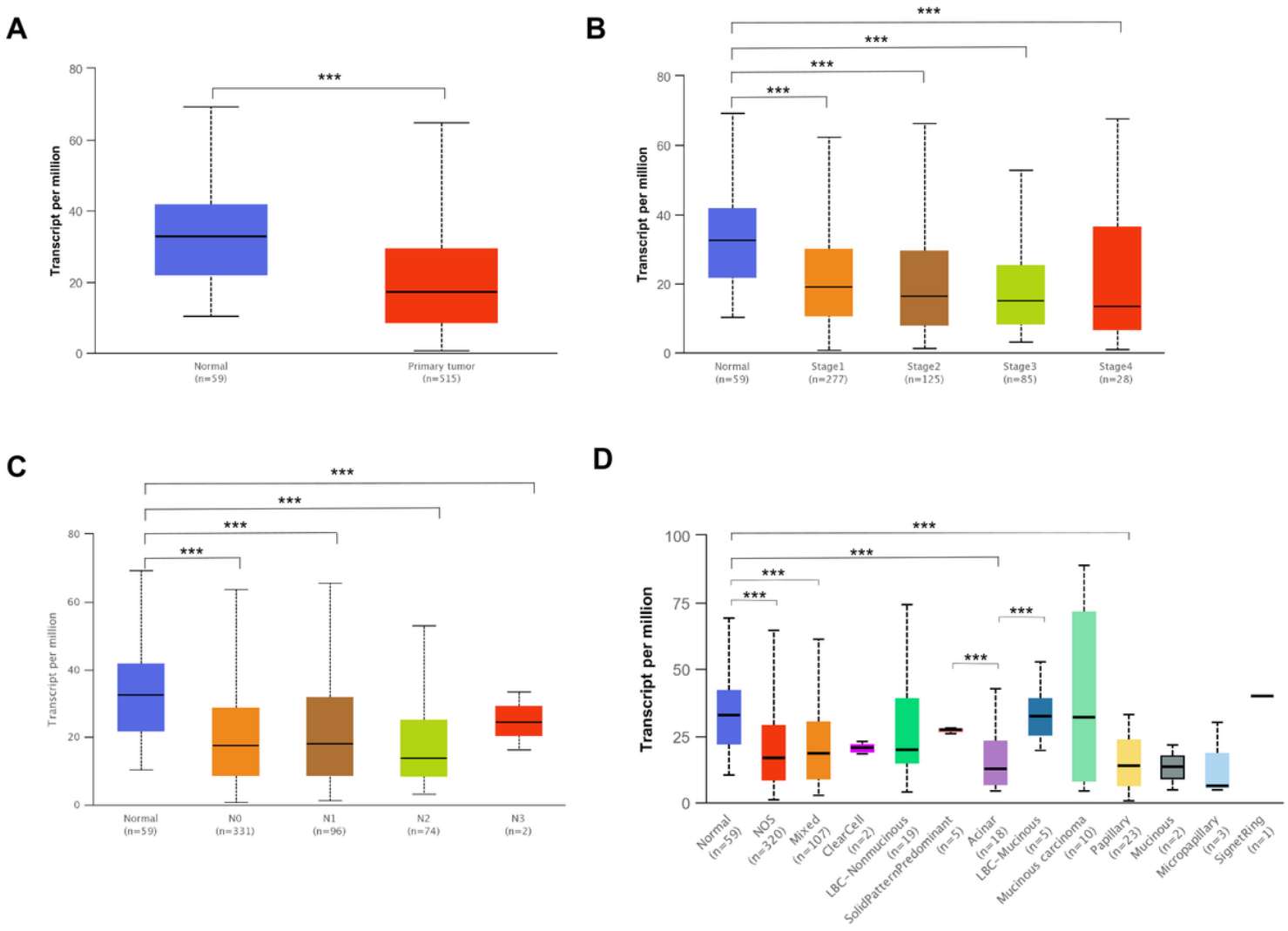

Figure 2

Correlation between *IGSF6* expression and LUAD clinicopathological parameters

(A) Sample type (normal/primary tumor). (B) Cancer stage (stage 1, 2, 3, and 4). (C) Lymph node stage (N0 1, 2, and 3). (D) LUAD subtypes. ***p<0.001.

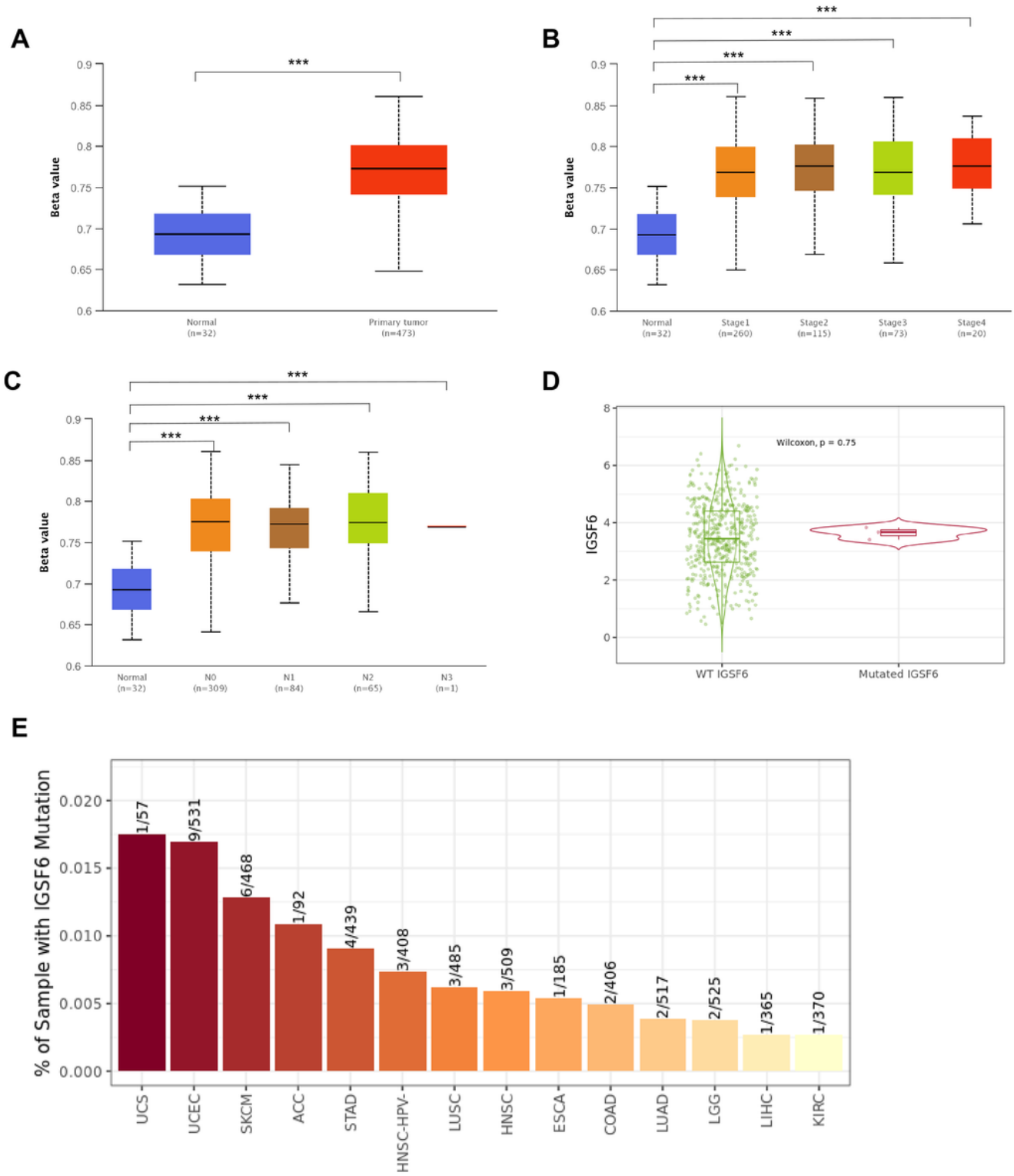

Figure 3

Correlation between promoter methylation level of *IGSF6* and LUAD clinicopathological parameters

(A) Sample type (normal/primary tumor). (B) Cancer stage (stage 1, 2, 3, and 4). (C) Lymph node stage (N0 1, 2, and 3). (D-E) *IGSF6* expression level in WT and *IGSF6*-mutated groups of LUAD. ***p<0.001.

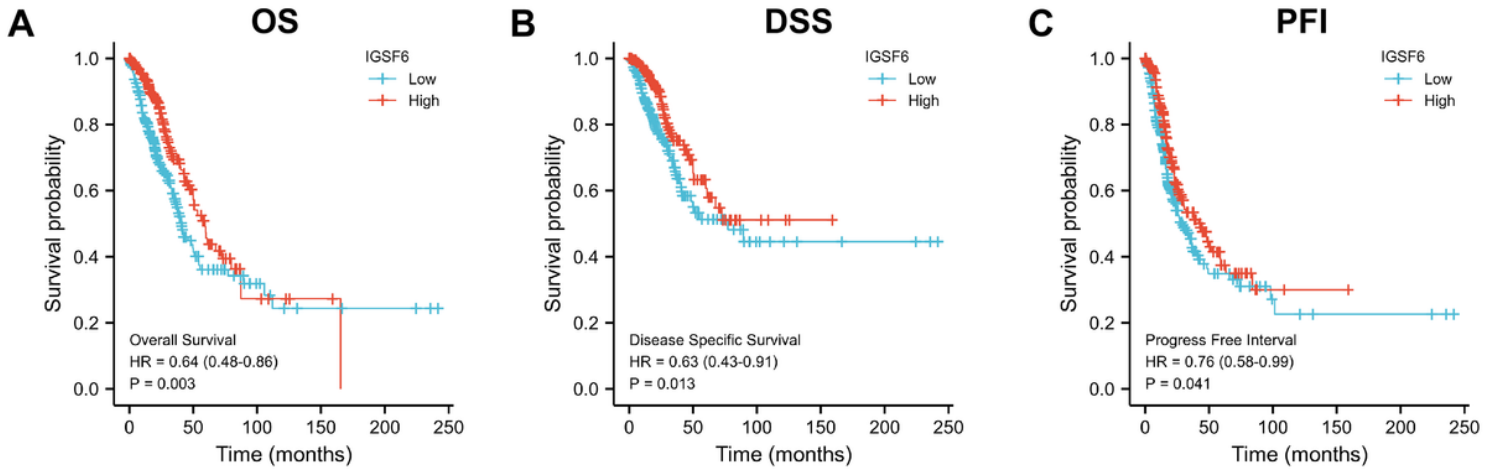

Figure 4

Correlation between *IGSF6* expression and LUAD prognosis

Kaplan–Meier survival curves comparing the high-*IGSF6* and low-*IGSF6* cohorts in LUAD, (A) OS, (B) DSS, and (C) PFI in LUAD.

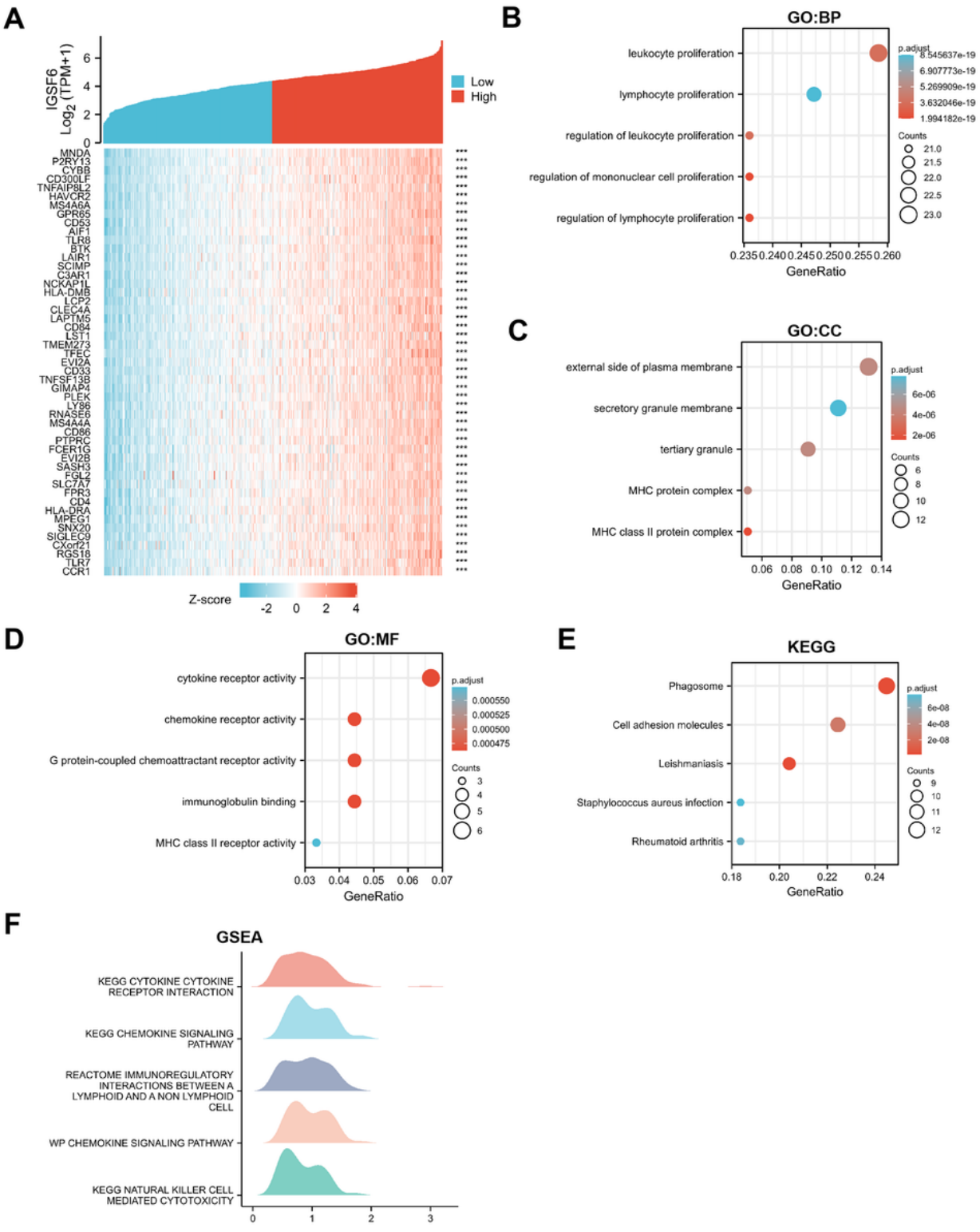

Figure 5

Correlation and enrichment analyses of *IGSF6*

(A) The correlation analysis of *IGSF6* in LUAD. Top 50 genes associated with *IGSF6*were shown in heatmap. Data were normalized by Z-score standardization method. (B-D) Enrichment analysis of *IGSF6*

in LUAD. Significant GO terms of top 300 genes most positively associated with *IGSF6*, including (B) BP, (C) CC, and (D) MF. (E) KEGG pathways. (F) GSEA results.

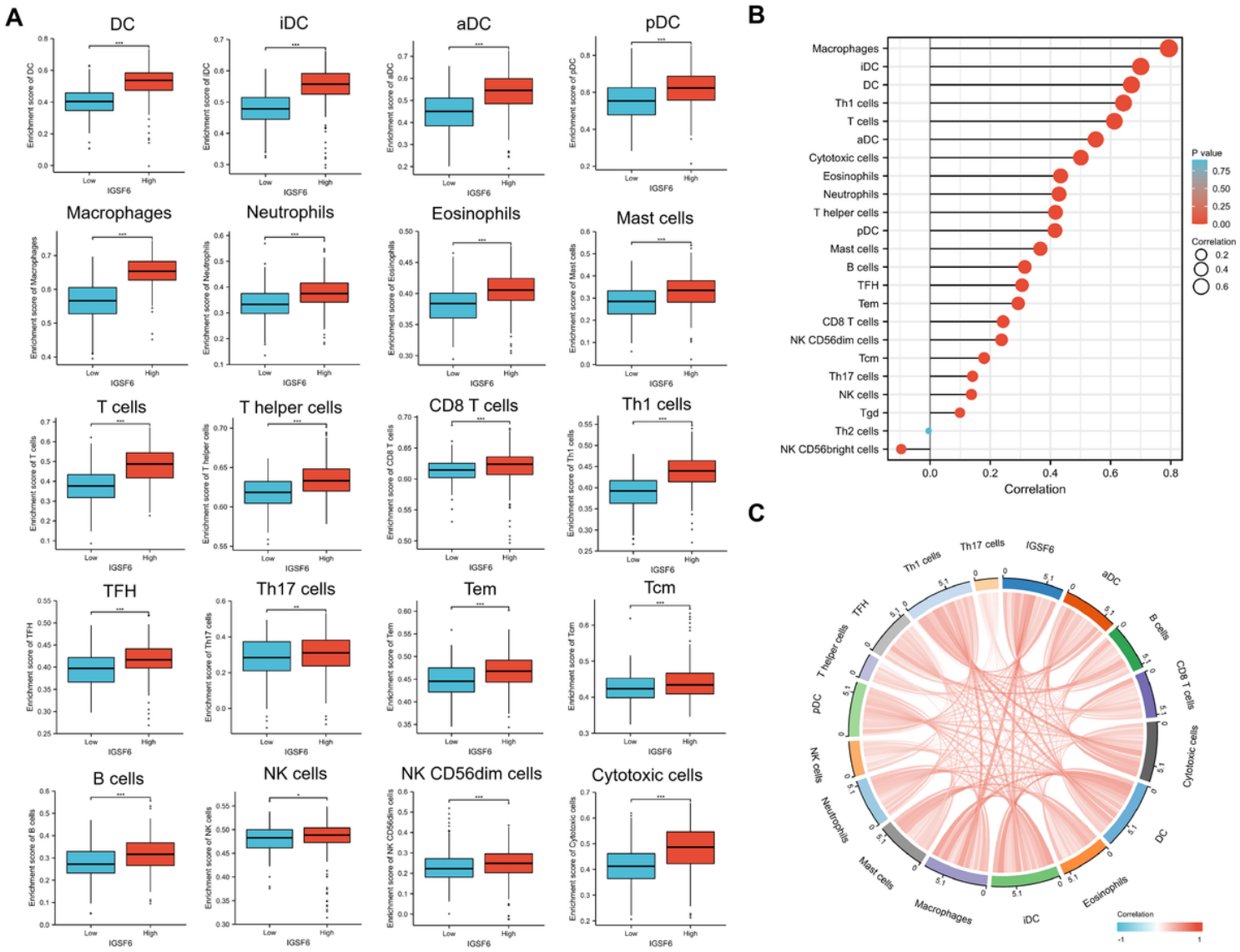

Figure 6

Correlation between *IGSF6* and immune cell infiltration in LUAD

(A) Infiltration scores of immune cells in high- and low-*IGSF6* expression groups in LUAD. (B-C) The correlation between *IGSF6* and the immune cell infiltration levels. Red represents positive correlation, blue represents negative correlation, and the deeper the color, the stronger the correlation. **p*< 0.05, ***p*< 0.01, ****p*< 0.001.

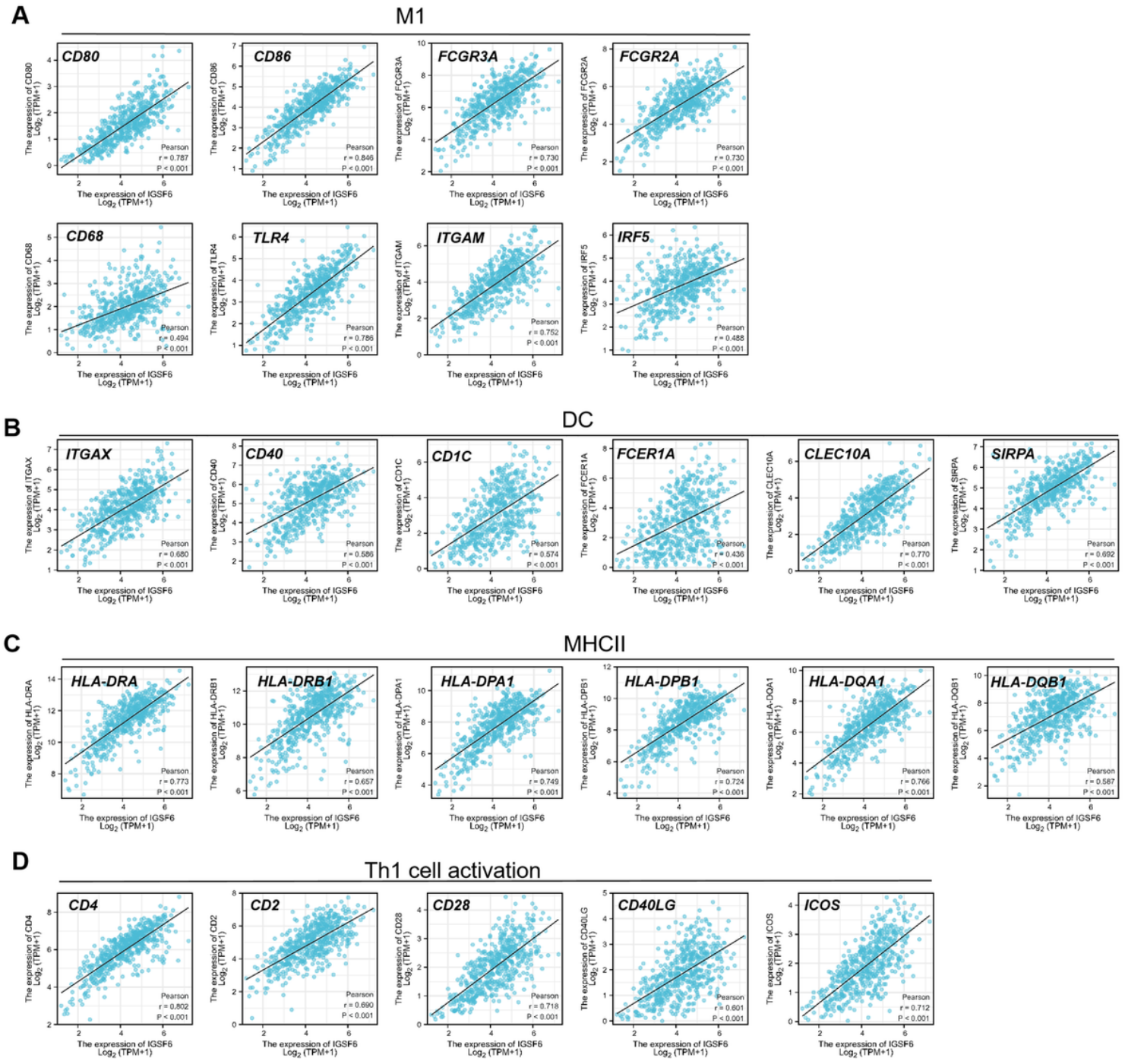

Figure 7

Association of *IGSF6* expression with molecular markers of M1, DCs, and Th1 activation in LUAD

Scatterplots of correlations between *IGSF6* expression and markers of (A) M1 (*CD80*, *CD86*, *FCGR3A*, *FCGR2A*, *CD68*, *TLR4*, *ITGAM*, and *IRF5*), (B) DCs (*ITGAX*, *CD40*, *CD1C*, *FCER1A*, *CLEC10A*, and *SIRPA*), and (C) MHCII (*HLA-DRA*, *HLA-DRB1*, *HLA-DPA1*, *HLA-DPB1*, *HLA-DQA1*, and *HLA-DQB1*), and (D) Th1 cell activation (*CD4*, *CD2*, *CD28*, *CD40LG*, and *ICOS*) in LUAD.

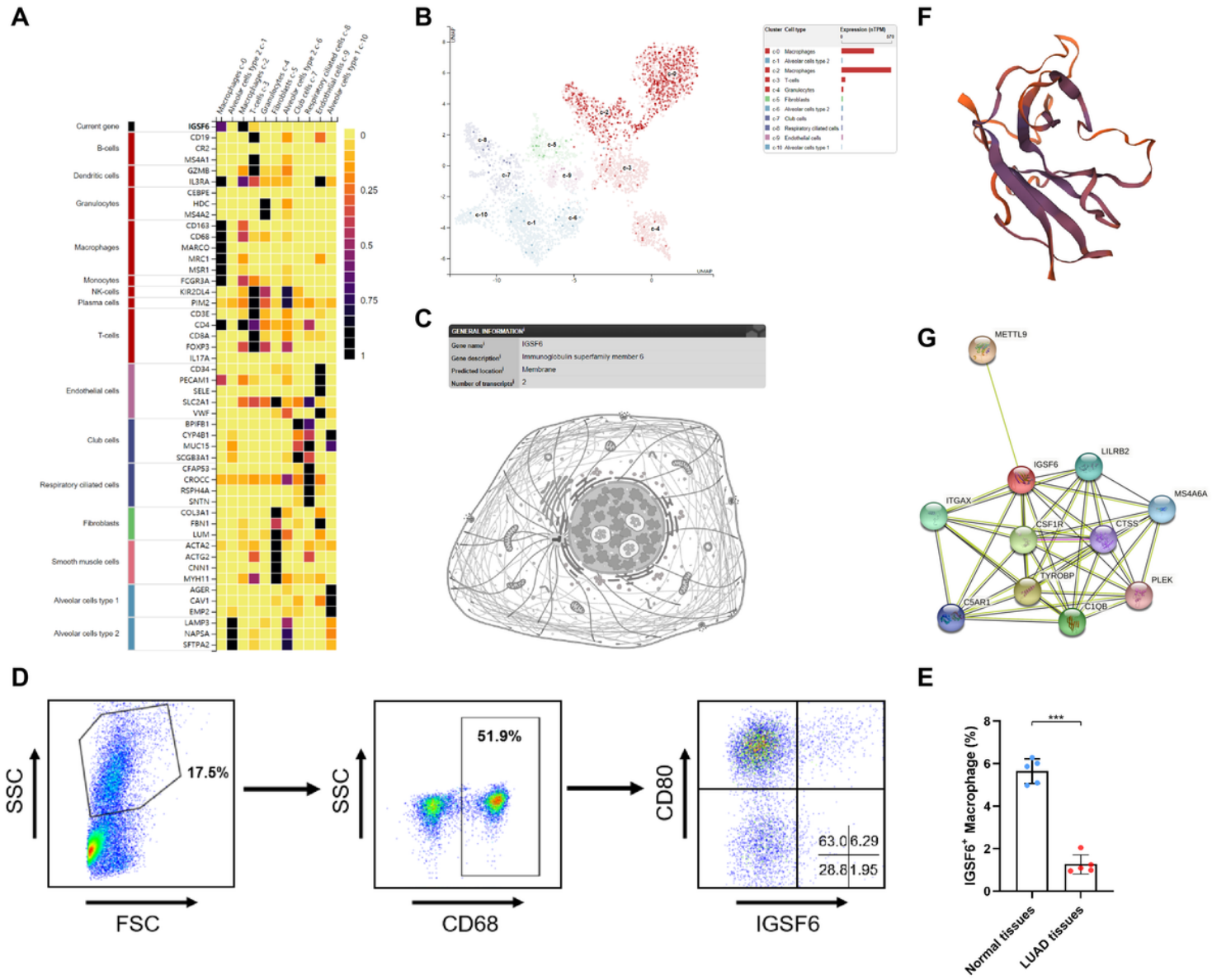

Figure 8

IGSF6 is localized on the membrane of macrophages in LUAD

(A) Heatmap representation of the expression correlation between *IGSF6* and different cell types in lung was obtained from HPA. (B) Analysis of IGSF6 level in different cell type groups derived from lung tissues. (C) Prediction of IGSF6 subcellular localization. (D-E) FCM was used to detect the IGSF6 protein located on the plasma membrane of macrophages from LUAD tissues and adjacent normal tissues of LUAD (n=5). (D) The gating strategy. (E) The proportion of $IGSF6^{+}$ macrophages in normal tissues and LUAD tissues (n=5). (F) Spatial conformation of the IGSF6 protein. (G) Functional protein association network analysis of IGSF6. Data were shown as mean ± SD. ***p< 0.001.

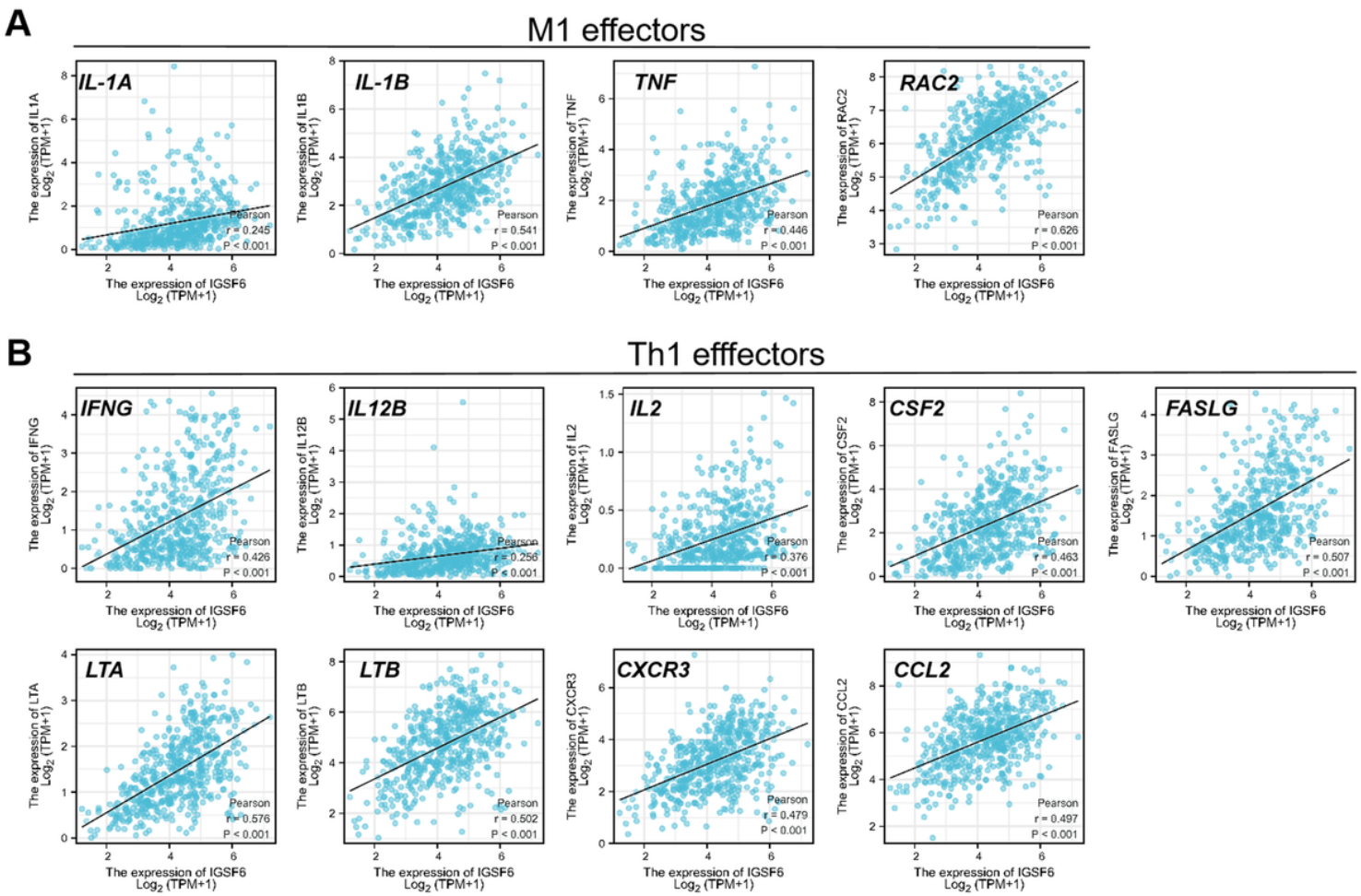

Figure 9

Correlation of *IGSF6*expression with effector molecules of M1 and Th1 cells in LUAD

Correlations between *IGSF6*expression and effector molecules of (A) M1 including *IL-1A*, *IL-1B*, *TNF*, and *RAC2*, (B) Th1 including *IFNG*, *IL12B*, *IL-2*, *CSF2*, *FASLG*, *LTA*, *LTB*, *CXCR3*, and *CCL2*in LUAD.

Supplementary Files

This is a list of supplementary files associated with this preprint. Click to download.

- SupplementaryFiles.pdf